URSI GASS 2021, Rome, Italy, 28 August - 4 September 2021

Spatial Evolution of Quantized Discrete-Mode Operators in a Lossy Nonlinear Josephson-Embedded Transmission Line

Yongjie Yuan*, Michael Haider, Johannes A. Russer, Peter Russer, and Christian Jirauschek
Department of Electrical and Computer Engineering, Technical University of Munich, Arcisstr. 21, 80333 Munich, Germany

Abstract

We present a description of the spatial evolution of quantized discrete-mode operators along a lossy nonlinear transmission line. The nonlinearity is formed by hundereds or even thousands of Josephson junctions which are placed periodically along a microwave transmission line. Dissipation is added to the system Hamiltonian by coupling the nonlinear transmission line to an Ohmic bath. Using the Hamiltonian of the open quantum system, Heisenberg equations of motion for the discrete mode operators can be derived in terms of quantum Langevin equations. The temporal equations of motion are then translated to the spatial domain to investigate the performance of a nonlinear four-wave-mixing process, while signals propagate along the transmission line.

1 Introduction

Superconducting microwave amplifiers are a key building block for the realization of high fidelity qubit readout circuits in ultra-low temperature quantum computers [1]. These amplifiers utilize Josephson junctions as nonlinear elements, where the amplification occurs due to a wave-mixing process. A Josephson junction is an arrangement of two superconductors that are weakly coupled across a thin insulating barrier [2, 3]. It has been demonstrated that Josephson junctions can be used for parametric amplification [4], microwave harmonic generation [5], and for the realization of quantum bits [6]. Josephson parametric amplifiers are particularly interesting for ultra-low noise applications, as their added noise approaches the quantum limit [7, 8]. To achieve a high parametric gain, the interaction time of the Josephson nonlinearity and the microwave signal needs to be maximized. One approach is to place a single Josephson junction inside a microwave cavity, which leads to an increased parametric gain in the reflected signal at the expense of instantaneous bandwidth [9]. A first quantum mechanical treatment of such a DC-pumped Josephson parametric amplifier (JPA) was given in [10]. Cavity losses and thermal noise in a quantum mechanical model of a JPA have been discussed in [11].

In a different architecture [12], the interaction time is maximized by periodically embedding Josephson junctions into a microwave transmission line, enabling parametric amplification of microwave signals along the propagation path. Such a Josephson traveling-wave parametric amplifier (JTWPA) avoids the bandwidth limitations imposed by a resonant cavity. The parametric amplification is, however, strongly phase-dependent, which requires proper dispersion engineering to achieve a sufficiently large gain [9]. The four-wave-mixing process in a resonantly phase-matched JTWPA can be described by a continous nonlinear wave equation [12], from which coupled mode equations can be derived for the amplitudes of the respective pump, signal, and idler contributions [9]. Quantum mechanical descriptions for a JTWPA are given in [13] and [14] for continous and discrete-mode quantization, respectively.

We have previously introduced noise and dissipation in a circuit quantum electrodynamic description of a JTWPA in [15]. There, we derived a quantum model for the temporal dynamics of a JTWPA including noise and dissipation due to the imperfect substrate insulation. However, because of the nonlinear dispersion, each individual mode spends a different amount of time traveling along the amplifier. Therefore, special care must be taken when considering co-rotating frames for the individual discrete mode operators. In this work, we circumvent this problem by considering the spatial evolution of the mode operators instead.

In section 2 we revisit the theory of parametric amplification and demonstrate how we model dissipation and fluctuation in terms of quantum reservoir theory. The quantum Langevin equations for the individual modes in the spatial domain are derived in section 3. After a series of approximations, we present an analytic solutions for the input-output relation of the signal mode. In section 4, we compare the results for the dissipative case to non-dissipative results from the literature.

2 JTWPA Model and Reservoir Coupling

We consider the nonlinear transmission line structure of a JTWPA as given in [12]. The circuit is implemented as a lumped element coplanar transmission line comprising hundereds or thousands of unit cells with a cell length of Δz. Each unit cell contains a single Josephson junction, where the Josephson junction capacitance is modeled by a parallel

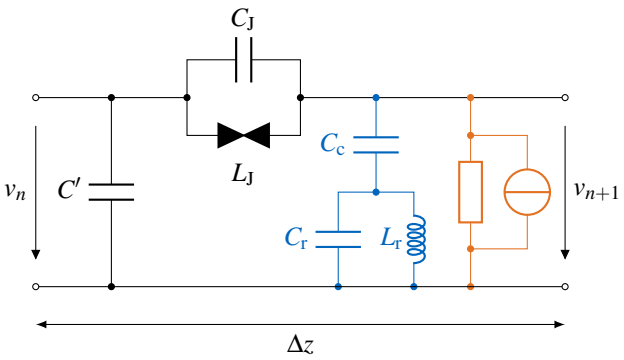

Figure 1. Unit cell of a JTWPA. The resonant phase matching circuit and a resistive representation of the bath is highlighted in blue and orange color, respectively. The bath adds noise to the system via the current source, and dissipates energy through the resistor.

capacitor C_J, while the line inductance is neglected compared to the Josephson inductance. The circuit diagram of the unit cell is given in Figure 1.

Parametric amplification is achieved through a wave-mixing process, where energy is transfered from a strong pump tone to the respective signal mode [16]. In a JTWPA, this process is a result of the nonlinear response of the Josephson inductance to the field passing through the transmission line [14]. Depending on the type of the nonlinear response [17], we distinguish between three- and four-wave-mixing. In the following, we consider non-degenerate four-wave-mixing with a degenerate pump mode. Due to self- and cross-phase-modulation there is a strong nonlinear contribution which is to be added to the linear dispersion. We use dispersion engineering to improve the amplifier's performance. A resonant phase shifter consisting of an LC-resonator and a coupling capacitor is added in each unit cell to achieve resonant phase-matching (RPM) [9].

The electric field propagating though a conventional transmission line experiences resistive and dielectric losses. The resistive dissipation occurs due to the finite conductivity of the material that forms the line, while the dielectric losses originate from the imperfect electric insulation of the substrate medium [18]. For superconducting traveling-wave parametric amplifiers, only dielectric losses need to be taken into account. In our quantum model of dissipation, a bath representing a photon field in thermal equilibrium is coupled to the system [19]. The bath consists of an infinite series of harmonic oscillators with densely spaced frequencies ω_n. The total Hamiltonian of the dissipative system with reservoir coupling is then given by $\hat{H}_{\text{total}} = \hat{H}_{\text{sys}} + \hat{H}_{\text{bath}} + \hat{H}_{\text{coupling}}$, where $\hat{H}_{\text{sys}}$ is the Hamiltonian of the unperturbed system, $\hat{H}_{\text{bath}}$ describes the heat bath, and $\hat{H}_{\text{coupling}}$ represents the system-reservoir interaction.

3 Spatial Evolution and Analytic Solution

We consider right-propagating discrete sinusoidal modes. The lossless system is described in terms of the discrete-mode operator Hamiltonian $\hat{H}^{\text{CP}}_{\text{TWPA}}$ from [14], assuming a strong classical pump current. As we consider signal energies in the range of single microwave photons, pump depletion due to the four-wave mixing process is neglected. We also neglect coupling of the pump mode with the dissipative bath. The resulting total Hamiltonian, as well as the respective equations of motion for the signal, idler, and pump modes, follow analogous to [15].

The temporal Heisenberg equations of motion are mapped to their spatial counterparts by the relation $-\omega_n \partial t = k_n \partial z$, where ω_n is the angular frequency of the n-th mode and k_n is the associated wave number. Hence, the spatial Heisenberg equations are given by

$$\partial_z \hat{a}_{\text{s}} = \text{i}\,(k_{\text{s}} + \delta_{\text{s}})\,\hat{a}_{\text{s}} - \text{i}\frac{k_{\text{s}}}{\omega_{\text{s}}}\chi' A_{\text{p}}^2 \hat{a}_{\text{i}}^\dagger + \text{i}\frac{k_{\text{s}}}{\omega_{\text{s}}}\sum_n g_{\text{s},n}\hat{b}_n\,, \quad (1)$$

$$\partial_z \hat{a}_{\text{i}} = \text{i}\,(k_{\text{i}} + \delta_{\text{i}})\,\hat{a}_{\text{i}} - \text{i}\frac{k_{\text{i}}}{\omega_{\text{i}}}\chi' A_{\text{p}}^2 \hat{a}_{\text{s}}^\dagger + \text{i}\frac{k_{\text{i}}}{\omega_{\text{i}}}\sum_n g_{\text{i},n}\hat{b}_n\,, \quad (2)$$

$$\partial_z \hat{b}_n = \text{i}k_n \hat{b}_n + \text{i}\frac{k_n}{\omega_n} g_{\text{s},n}\hat{a}_{\text{s}} + \text{i}\frac{k_n}{\omega_n} g_{\text{i},n}\hat{a}_{\text{i}}\,, \quad (3)$$

where $\hat{a}_{\text{j}}^\dagger$ and $\hat{a}_{\text{j}}$ with $j \in \{\text{s},\text{i}\}$ are the respective creation and annihilation operators for a photon in the signal or idler mode, χ' is the four-wave-mixing interaction strength as given in [14], and $\delta_j = k_j \xi_j' |A_{\text{p},0}|^2/\omega_j$, where ξ_j' are coefficients related to the critical current of the Josephson junction and to the dispersion relation, with $j \in \{\text{s},\text{i},\text{p}\}$.

The classical pump amplitude A_{p} evolves according to

$$\partial_z A_{\text{p}} = \text{i}\left(k_{\text{p}} + 2\delta_{\text{p}}\right) A_{\text{p}}\,, \quad (4)$$

which can be solved analytically. By a formal integration of (3), we obtain the bath operators $\hat{b}_n$ in terms of the system operators and random zero-mean fluctuations $\hat{b}_{n,0}$. Inserting the formal integral into (1) and (2), we obtain a system of two coupled operator equations of motion, containing randomly fluctuating terms. We switch to a co-rotating frame $\hat{A}_j = \hat{a}_j \text{e}^{-\text{i}\left(k_j + \delta_j + \Delta k_{\text{T}}/2\right)z}$, with $j \in \{\text{s},\text{i}\}$ in order to simplify the resulting equations. The total phase mismatch Δk_{T} is defined by

$$\Delta k_{\text{T}} = 2k_{\text{p}} - k_{\text{s}} - k_{\text{i}} + 2\delta_{\text{p}} - \delta_{\text{s}} - \delta_{\text{i}}\,. \quad (5)$$

In a next step, we replace the summation over infinitely many densely spaced modes in (1) and (2) by an integration over the wave-vector dependent one-dimensional density of states $\mathscr{D}(k)$, assuming a Markovian memory-less system [19]. Dropping all fast oscillating terms at non-resonant frequencies, the spatial Heisenberg equations of motion are given by

$$\partial_z \hat{A}_{\text{s}} = -\left(\frac{\gamma_{\text{s}}}{2} + \text{i}\frac{\Delta k_{\text{T}}}{2}\right)\hat{A}_{\text{s}} - \text{i}\frac{k_{\text{s}}}{\omega_{\text{s}}}\chi' A_{\text{p},0}^2 \hat{A}_{\text{i}}^\dagger + \hat{f}_{\text{s}}\,, \quad (6)$$

$$\partial_z \hat{A}_{\text{i}} = -\left(\frac{\gamma_{\text{i}}}{2} + \text{i}\frac{\Delta k_{\text{T}}}{2}\right)\hat{A}_{\text{i}} - \text{i}\frac{k_{\text{i}}}{\omega_{\text{i}}}\chi' A_{\text{p},0}^2 \hat{A}_{\text{s}}^\dagger + \hat{f}_{\text{i}}\,, \quad (7)$$

with the damping factors γ_s and γ_i [19]

$$\gamma_\mathrm{s} = 2\pi\mathscr{D}(k_\mathrm{s})g_\mathrm{s}^2(k_\mathrm{s})\frac{k_\mathrm{s}^2}{\omega_\mathrm{s}^2}, \quad \gamma_\mathrm{i} = 2\pi\mathscr{D}(k_\mathrm{i})g_\mathrm{i}^2(k_\mathrm{i})\frac{k_\mathrm{i}^2}{\omega_\mathrm{i}^2}. \tag{8}$$

The noise operators $\hat{f}_\mathrm{s}$ and $\hat{f}_\mathrm{i}$ in (6) and (7) result in

$$\hat{f}_\mathrm{s} = \mathrm{i}\frac{k_\mathrm{s}}{\omega_\mathrm{s}}\sum_n g_{\mathrm{s},n}\hat{b}_{n,0}\mathrm{e}^{\mathrm{i}\left(k_n - k_\mathrm{s} - \delta_\mathrm{s} - \frac{\Delta k_\mathrm{T}}{2}\right)z}, \tag{9}$$

$$\hat{f}_\mathrm{i} = \mathrm{i}\frac{k_\mathrm{i}}{\omega_\mathrm{i}}\sum_n g_{\mathrm{i},n}\hat{b}_{n,0}\mathrm{e}^{\mathrm{i}\left(k_n - k_\mathrm{i} - \delta_\mathrm{i} - \frac{\Delta k_\mathrm{T}}{2}\right)z}. \tag{10}$$

The system of coupled first-order differential equations can be solved analytically with standard methods. The annihilation operator of the signal mode is given by

$$\begin{aligned}\hat{A}_\mathrm{s} = &\left\{\left[\cosh(gz) + \frac{-\gamma_\mathrm{s} + \gamma_\mathrm{i} - 2\mathrm{i}\Delta k_\mathrm{T}}{4g}\sinh(gz)\right]\hat{A}_{\mathrm{s},0}\right.\\ &\left. - \frac{\mathrm{i}\frac{k_\mathrm{s}}{\omega_\mathrm{s}}\chi' A_{\mathrm{p},0}^2}{g}\sinh(gz)\hat{A}_{\mathrm{i},0}^\dagger\right\}\mathrm{e}^{-\frac{\gamma_\mathrm{s}+\gamma_\mathrm{i}}{4}z}\\ &+ \frac{k_\mathrm{s}}{\omega_\mathrm{s}}\sum_n g_{\mathrm{s},n}\hat{b}_{n,0}\left[\eta_+(k_n) - \eta_-(k_n)\right]\mathrm{e}^{\mathrm{i}\left(k_n - k_\mathrm{s} - \delta_\mathrm{s} - \frac{\Delta k_\mathrm{T}}{2}\right)z}\\ &+ \frac{k_\mathrm{s}}{\omega_\mathrm{s}}\sum_n g_{\mathrm{s},n}\hat{b}_{n,0}\left[\eta_-(k_n)\mathrm{e}^{gz} - \eta_+(k_n)\mathrm{e}^{-gz}\right]\mathrm{e}^{-\frac{\gamma_\mathrm{s}+\gamma_\mathrm{i}}{4}z}\\ &+ \frac{k_\mathrm{i}}{\omega_\mathrm{i}}\sum_n g_{\mathrm{i},n}^*\hat{b}_{n,0}^\dagger\left[\rho_+(k_n) - \rho_-(k_n)\right]\mathrm{e}^{-\mathrm{i}\left(k_n - k_\mathrm{i} - \delta_\mathrm{i} - \frac{\Delta k_\mathrm{T}}{2}\right)z}\\ &+ \frac{k_\mathrm{i}}{\omega_\mathrm{i}}\sum_n g_{\mathrm{i},n}^*\hat{b}_{n,0}^\dagger\left[\rho_-(k_n)\mathrm{e}^{gz} - \rho_+(k_n)\mathrm{e}^{-gz}\right]\mathrm{e}^{-\frac{\gamma_\mathrm{s}+\gamma_\mathrm{i}}{4}z},\end{aligned} \tag{11}$$

where we introduce the gain factor

$$g = \sqrt{\frac{(\gamma_\mathrm{s} - \gamma_\mathrm{i} + 2\mathrm{i}\Delta k_\mathrm{T})^2}{16} + \frac{k_\mathrm{s}}{\omega_\mathrm{s}}\frac{k_\mathrm{i}}{\omega_\mathrm{i}}|\chi'|^2\left|A_{\mathrm{p},0}^2\right|^2}, \tag{12}$$

and the coefficient functions

$$\eta_\pm(k) = \frac{\mathrm{i}}{2g}\frac{\gamma_\mathrm{s} - \gamma_\mathrm{i} + 2\mathrm{i}\Delta k_\mathrm{T} \pm 4g}{\pm 4g + \gamma_\mathrm{s} + \gamma_\mathrm{i} + 4\mathrm{i}\left(k - k_\mathrm{s} - \delta_\mathrm{s} - \frac{\Delta k_\mathrm{T}}{2}\right)}, \tag{13}$$

$$\rho_\pm(k) = \frac{1}{g}\frac{2\frac{k_\mathrm{s}}{\omega_\mathrm{s}}\chi' A_{\mathrm{p},0}^2}{\pm 4g + \gamma_\mathrm{s} + \gamma_\mathrm{i} - 4\mathrm{i}\left(k - k_\mathrm{i} - \delta_\mathrm{i} - \frac{\Delta k_\mathrm{T}}{2}\right)}. \tag{14}$$

The first and second lines in (11) are related to the four-wave-mixing induced parametric amplification. Dissipation is taken into account by the exponential damping term, depending on the damping factors γ_s and γ_i. The last four lines contain the contributions of thermal noise photons. Our solution to the signal annihilation operator is similar to [20]. There, however, the noise contributions due to the signal-bath coupling are not given explicitly. The coupling constants $g_{\mathrm{s},n}$ are chosen to form an Ohmic bath [21], modeling the dielectric losses along the transmission line due to the imperfect substrate insulation.

From the analytic solution of the signal photon annihilation operator, we can calculate the average photon number at any spatial location along the JTWPA nonlinear transmission line. Neglecting the noise contributions, the expected number of signal photons at a certain spatial location z is given by

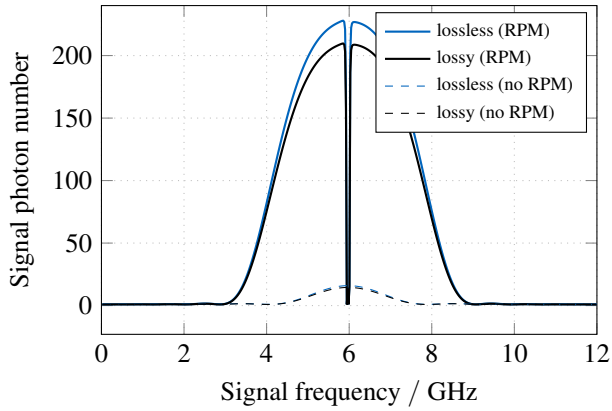

Figure 2. Comparison of the signal photon number at the output of a JTWPA for the dissipative and non-dissipative case, with and without RPM. The Josephson capacitance $C_\mathrm{J} = 329\,\mathrm{fF}$ and the critical current $I_\mathrm{c} = 3.29\,\mu\mathrm{A}$.

$$\begin{aligned}\left\langle\hat{A}_\mathrm{s}^\dagger\hat{A}_\mathrm{s}\right\rangle = &\left[\left|\cosh(gz) + \frac{-\gamma_\mathrm{s} + \gamma_\mathrm{i} - 2\mathrm{i}\Delta k_\mathrm{T}}{4g}\sinh(gz)\right|^2 \times\right.\\ &\times\left\langle\hat{A}_{\mathrm{s},0}^\dagger\hat{A}_{\mathrm{s},0}\right\rangle + \left|\frac{k_\mathrm{s}}{\omega_\mathrm{s}}\frac{\chi' A_{\mathrm{p}0}^2}{g}\sinh(gz)\right|^2 \times\\ &\times\left(\left\langle\hat{A}_{\mathrm{i},0}^\dagger\hat{A}_{\mathrm{i},0}\right\rangle + 1\right) - \mathrm{i}\zeta(z)\left\langle\hat{A}_{\mathrm{s},0}^\dagger\hat{A}_{\mathrm{i},0}^\dagger\right\rangle\\ &\left. + \mathrm{i}\zeta^*(z)\left\langle\hat{A}_{\mathrm{s},0}\hat{A}_{\mathrm{i},0}\right\rangle\right]\mathrm{e}^{-\frac{\gamma_\mathrm{s}+\gamma_\mathrm{i}}{2}z},\end{aligned} \tag{15}$$

where the correlations $\left\langle\hat{A}_{\mathrm{s},0}^\dagger\hat{A}_{\mathrm{i},0}^\dagger\right\rangle$ and $\left\langle\hat{A}_{\mathrm{s},0}\hat{A}_{\mathrm{i},0}\right\rangle$ enter as factors of

$$\begin{aligned}\zeta(z) = &\left[\cosh(gz) + \frac{-\gamma_\mathrm{s} + \gamma_\mathrm{i} - 2\mathrm{i}\Delta k_\mathrm{T}}{4g}\sinh(gz)\right]^* \times\\ &\times\frac{k_\mathrm{s}}{\omega_\mathrm{s}}\frac{\chi' A_{\mathrm{p},0}^2}{g}\sinh(gz).\end{aligned} \tag{16}$$

It can be shown that those correlations vanish, if either the signal or the idler mode is initially given as a number state.

4 Evolution of the Signal Photon Number

In Figure 2, the finite substrate resistance becomes visible when comparing the average number of photons in the signal mode after propagating through a JTWPA of length l with the ideal case, assuming a perfectly insulating substrate. We predict the average number of signal photons by evaluating (15) with the parameters from [14]. The photon number is evaluated for different signal modes with frequencies f_s, with and without RPM. At the input, we assume a single photon in the signal mode and no idler photons. The pump frequency is kept constant at 5.97 GHz with

a pump current of $I_p = 0.5 I_c$. The signal frequency is varied in a range from 0 GHz to 12 GHz. The total length of the nonlinear transmission line is chosen to be 20 mm, where the line impedance is $\approx 50\,\Omega$. Damping factors are chosen in the range of $4\,\mathrm{m}^{-1}$ to $5\,\mathrm{m}^{-1}$.

5 Conclusion

We have presented a model for the spatial evolution of discrete-mode operators based on the mesoscopic Hamiltonian from [14], including noise and dissipation. A closed-form analytic solution has been derived, and used to predict the expectation value of the signal photon number at the output of a JTWPA. The signal photon number at the output of the JTWPA has contributions from the four-wave-mixing process and the down-converted idler photons. The signal mode experiences exponential damping from the system-bath interaction. The difference in the output photon number when considering imperfect substrate insulation has been visualized using an examplary JTWPA structure. The spatial system dynamics have been investigated assuming a classical undepleted pump mode. In the scope of further research, we propose to take pump losses into account, as the gain coefficient is directly proportional to the pump amplitude.

References

[1] C. A. Ryan, B. R. Johnson, D. Risté, B. Donovan, and T. A. Ohki, "Hardware for dynamic quantum computing," *Rev. Sci. Instrum.*, vol. 88, no. 10, p. 104703, 2017.

[2] B. D. Josephson, "Possible new effects in superconductive tunnelling," *Phys. Lett.*, vol. 1, no. 7, pp. 251–253, 1962.

[3] K. K. Likharev, "Superconducting weak links," *Rev. Mod. Phys.*, vol. 51, pp. 101–159, 1979.

[4] P. Russer, "Parametric amplification with Josephson junctions," *Arch. Elektr. Uebertrag.*, vol. 23, no. 8, pp. 417–420, 1969.

[5] S. Shapiro, "Microwave harmonic generation from Josephson junctions," *J. Appl. Phys.*, vol. 38, pp. 1879–1884, 1967.

[6] A. Shnirman, G. Schön, and Z. Hermon, "Quantum manipulations of small Josephson junctions," *Phys. Rev. Lett.*, vol. 79, pp. 2371–2374, 1997.

[7] C. M. Caves, "Quantum limits on noise in linear amplifiers," *Phys. Rev. D*, vol. 26, pp. 1817–1839, 1982.

[8] C. Eichler, Y. Salathe, J. Mlynek, S. Schmidt, and A. Wallraff, "Quantum-limited amplification and entanglement in coupled nonlinear resonators," *Phys. Rev. Lett.*, vol. 113, p. 110502, 2014.

[9] K. O'Brien, C. Macklin, I. Siddiqi, and X. Zhang, "Resonant phase matching of Josephson junction traveling wave parametric amplifiers," *Phys. Rev. Lett.*, vol. 113, p. 157001, 2014.

[10] F. X. Kaertner and P. Russer, "Generation of squeezed microwave states by a dc-pumped degenerate parametric Josephson junction oscillator," *Phys. Rev. A*, vol. 42, pp. 5601–5612, 1990.

[11] W. Kaiser, M. Haider, J. A. Russer, P. Russer, and C. Jirauschek, "Quantum theory of the dissipative Josephson parametric amplifier," *Int. J. Circ. Theor. App.*, vol. 45, no. 7, pp. 864–881, 2017.

[12] O. Yaakobi, L. Friedland, C. Macklin, and I. Siddiqi, "Parametric amplification in Josephson junction embedded transmission lines," *Phys. Rev. B*, vol. 87, p. 144301, 2013.

[13] A. L. Grimsmo and A. Blais, "Squeezing and quantum state engineering with Josephson travelling wave amplifiers," *npj Quantum Inf.*, vol. 3, pp. 1–10, 2017.

[14] T. H. A. van der Reep, "Mesoscopic Hamiltonian for Josephson traveling-wave parametric amplifiers," *Phys. Rev. A*, vol. 99, p. 063838, 2019.

[15] Y. Yuan, M. Haider, J. A. Russer, P. Russer, and C. Jirauschek, "Noise and dissipation in a circuit quantum electrodynamic description of a Josephson traveling-wave parametric amplifier," in *XXXIIIrd General Assembly and Scientific Symposium of the International Union of Radio Science*, 2020, pp. 1–4.

[16] G. P. Agrawal, *Nonlinear fiber optics*, 3rd ed. Academic Press, 2001.

[17] A. B. Zorin, "Josephson traveling-wave parametric amplifier with three-wave mixing," *Phys. Rev. Applied*, vol. 6, p. 034006, 2016.

[18] J. R. Zurita-Sánchez and C. Henkel, "Lossy electrical transmission lines: Thermal fluctuations and quantization," *Phys. Rev. A*, vol. 73, no. 6, p. 063825, 2006.

[19] M. Sargent, M. O. Scully, and W. E. Lamb, *Laser Physics*. Boston: Addison-Wesley Press, 1974.

[20] M. Houde, L. C. G. Govia, and A. A. Clerk, "Loss asymmetries in quantum traveling-wave parametric amplifiers," *Phys. Rev. Applied*, vol. 12, p. 034054, 2019.

[21] U. Vool and M. Devoret, "Introduction to quantum electromagnetic circuits," *Int. J. Circ. Theor. App.*, vol. 45, no. 7, pp. 897–934, 2017.